AD-A040 090 NAVAL RESEARCH LAB WASHINGTON D C F/G 20/9
TWO-DIMENSIONAL FLUID SIMULATION OF RELATIVISTIC ELECTRON BEAM---ETC(U)
MAY 77 D G COLOMBANT, D MOSHER

UNCLASSIFIED NRL-MR-3496 NL

| OF |
AD
A040 090

END
DATE FILMED
6-77

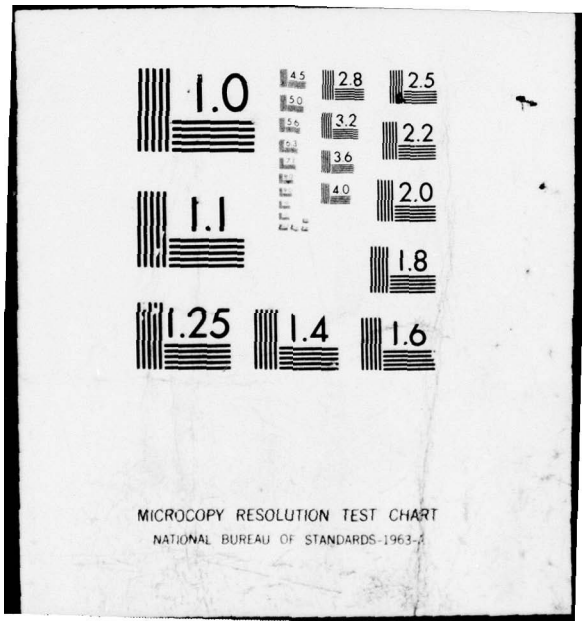
1.0
1.1
1.25
1.4
1.6
1.8
2.0
2.2
2.5
2.8
3.2
3.6
4.0
4.5
5.0
5.6
MICROCOPY RESOLUTION TEST CHART
NATIONAL BUREAU OF STANDARDS-1963-A

NRL Memorandum Report 3496

Two-Dimensional Fluid Simulation of Relativistic Electron Beam-High Z Target Interactions

D. G. COLOMBANT and D. MOSHER

Plasma Dynamics Branch
Plasma Physics Division

May 1977

This research was sponsored by the Defense Nuclear Agency under subtask T99QAXLA014, work unit 05, and work unit title Advanced Concepts.

NAVAL RESEARCH LABORATORY
Washington, D.C.

SECURITY CLASSIFICATION OF THIS PAGE (When Data Entered)

REPORT DOCUMENTATION PAGE

READ INSTRUCTIONS BEFORE COMPLETING FORM

1. REPORT NUMBER: NRL Memorandum Report 3496	2. GOVT ACCESSION NO.
3. RECIPIENT'S CATALOG NUMBER	
4. TITLE (and Subtitle): TWO-DIMENSIONAL FLUID SIMULATION OF RELATIVISTIC ELECTRON BEAM-HIGH Z TARGET INTERACTIONS	5. TYPE OF REPORT & PERIOD COVERED: Interim report on a continuing NRL problem.
	6. PERFORMING ORG. REPORT NUMBER
7. AUTHOR(s): D.G. Colombant and D. Mosher	8. CONTRACT OR GRANT NUMBER(s)
9. PERFORMING ORGANIZATION NAME AND ADDRESS: Naval Research Laboratory, Washington, D.C. 20375	10. PROGRAM ELEMENT, PROJECT, TASK AREA & WORK UNIT NUMBERS: NRL Problem H02-26K, T99QAXLA014
11. CONTROLLING OFFICE NAME AND ADDRESS: Defense Nuclear Agency, Washington, D.C. 20305	12. REPORT DATE: May 1977
	13. NUMBER OF PAGES: 24
14. MONITORING AGENCY NAME & ADDRESS (if different from Controlling Office)	15. SECURITY CLASS. (of this report): UNCLASSIFIED
	15a. DECLASSIFICATION/DOWNGRADING SCHEDULE

16. DISTRIBUTION STATEMENT (of this Report)

Approved for public release; distribution unlimited.

17. DISTRIBUTION STATEMENT (of the abstract entered in Block 20, if different from Report)

18. SUPPLEMENTARY NOTES

This research was sponsored by the Defense Nuclear Agency under subtask T99QAXLA014, work unit 05, and work unit title Advanced Concepts.

19. KEY WORDS (Continue on reverse side if necessary and identify by block number)

Relativistic e-beam
Two-dimensional fluid simulation
Diode flow
Pinch formation

20. ABSTRACT (Continue on reverse side if necessary and identify by block number)

A two-dimensional r-z fluid code has been developed to study the interaction between a relativistic electron beam and an anode plasma. A self-consistent treatment of the electromagnetic fields has been included. Radial pinching of the beam is observed when its self-field resistively diffuses into the plasma.

DD FORM 1 JAN 73 1473 EDITION OF 1 NOV 65 IS OBSOLETE S/N 0102-014-6601

SECURITY CLASSIFICATION OF THIS PAGE (When Data Entered)

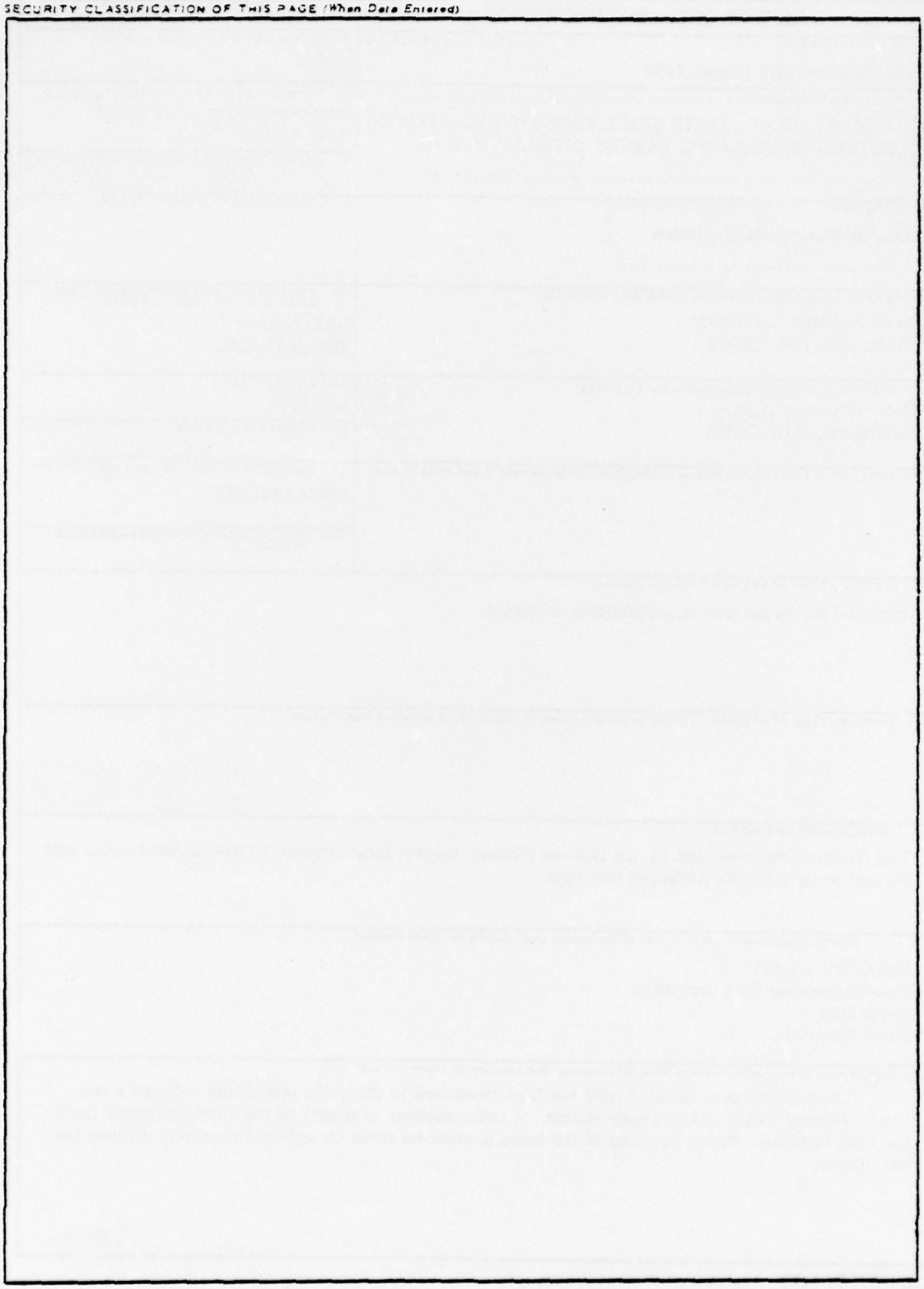

CONTENTS

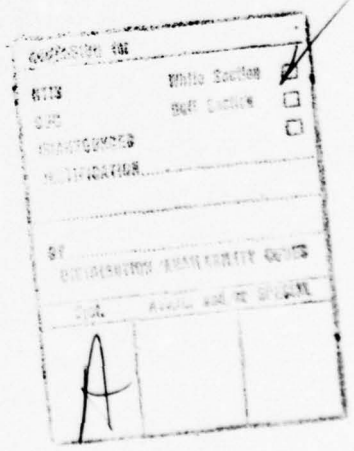

TWO DIMENSIONAL FLUID SIMULATION OF RELATIVISTIC ELECTRON BEAM-HIGH Z TARGET INTERACTIONS

I. INTRODUCTION

Calculations of pinched flows in relativistic electron beam diodes have so far relied heavily on particle simulation codes.[1-3] However, another possible approach consists of treating the electron beam as a fluid along with the anode plasma. Both approaches might be complementary in the understanding of mechanisms taking place inside the diodes.

In particular, Refs. 2 and 3 have been highly successful in explaining the pinching of the electron beam by bootstrapping its way toward the axis of the diode, showing how anode ions and plasma aid in the pinch formation. However, these works make specific, simple assumptions concerning the electromagnetic fields and the motion of the anode plasma.

It is clear that a fully self-consistent two-dimensional model of a relativistic electron beam-plasma interaction is desired. In this present work, we report on the numerical study of such an interaction by means of a two-dimensional fluid model. In this first attempt, we have made simplifying assumptions (convenient for a fluid model) and in particular, it is assumed that the plasma is low enough in density to neglect beam-plasma collisions so that the electrons can be treated as

Note: Manuscript submitted April 12, 1977.

cold. Calculations start when the self-field of the beam starts to diffuse into the plasma. It is desired to determine how charge-neutralization provided by the plasma causes the incident beam to pinch in the diffused magnetic field.

In Sec. II, a general model for the relativistic e-beam plasma interaction is presented as well as initial and boundary conditions. The general model includes collisions of the beam with the plasma. Simplified equations solved in the remainder of this study are then presented and their limits of application discussed. In Sec. III, the computational results obtained are displayed. In Sec. IV, conclusions are summarized and further steps are suggested in order to solve the full set of general equations.

II. MODEL EQUATIONS

Relativistic, collisional electron beam-plasma equations have been derived and reported by Mosher.[4] They are presented here again for the sake of completeness. If n denotes the beam electron density, $\underset{\sim}{u}$ its fluid-flow velocity, $\langle\gamma\rangle$ the value of γ (the relativistic factor) averaged over the beam electron distribution function, α_e and α_i the effective values of $Z \ln \Lambda_e$ and $Z^2 \ln \Lambda_i$ for interaction with plasma electrons and ions respectively, then the beam fluid equations can be written:

$$\frac{\partial n}{\partial t} + \underset{\sim}{\nabla} \cdot n\underset{\sim}{u} = 0 \ , \tag{1}$$

$$\frac{\partial \underset{\sim}{u}}{\partial t} + \underset{\sim}{u} \cdot \underset{\sim}{\nabla}\underset{\sim}{u} + \frac{1}{m_o \langle \gamma \rangle n} \underset{\sim}{\nabla} \cdot \underset{\approx}{\pi} + \frac{e}{m_o \langle \gamma \rangle} \left[\underset{\sim}{E} \cdot \left(\underset{\approx}{I} - \frac{\underset{\sim}{u}\underset{\sim}{u}}{c^2} \right) + \underset{\sim}{u} \times \underset{\sim}{B} \right]$$

$$= - 4\pi n_i r_o^2 c(\alpha_e + 2\alpha_i) \frac{\langle \gamma \rangle \underset{\sim}{u}}{\langle p \rangle^3 / m_o^3 c^3} , \qquad (2)$$

and

$$\frac{\partial \langle \gamma \rangle}{\partial t} + \underset{\sim}{u} \cdot \underset{\sim}{\nabla} \langle \gamma \rangle + \frac{e}{m_o c^2} \underset{\sim}{E} \cdot \underset{\sim}{u} = - 4\pi n_i r_o^2 c \alpha_e \frac{\langle \gamma \rangle}{\langle p \rangle / m_o c} , \qquad (3)$$

where π is a pressure term defined as

$$\underset{\approx}{\pi} = \frac{n \langle (\underset{\sim}{p} - \langle \underset{\sim}{p} \rangle)(\underset{\sim}{p} - \langle \underset{\sim}{p} \rangle) \rangle}{m_o \langle \gamma \rangle} ,$$

and

$$\langle p \rangle = mc(\langle \gamma \rangle^2 - 1)^{1/2} .$$

Appropriate forms for $\underset{\approx}{\pi}$ have been discussed.[4] The plasma equations coupled to these beam equations are:

$$\frac{\partial n_i}{\partial t} + \underset{\sim}{\nabla} \cdot n_i \underset{\sim}{v} = 0 , \qquad (4)$$

$$m_i n_i \left(\frac{\partial \underset{\sim}{v}}{\partial t} + \underset{\sim}{v} \cdot \underset{\sim}{\nabla}\underset{\sim}{v} \right) + \underset{\sim}{\nabla} p = \underset{\sim}{j} \times \underset{\sim}{B} , \qquad (5)$$

$$\frac{\partial \mathcal{E}}{\partial t} + \underset{\sim}{\nabla} \cdot \left[(\mathcal{E} + p) \underset{\sim}{v} \right] + \underset{\sim}{\nabla} \cdot \underset{\sim}{q} = \underset{\sim}{j} \cdot \underset{\sim}{E} - P_R$$

$$+ 4\pi n_i r_o^2 c \alpha_e \frac{\langle \gamma \rangle n m_o c^2}{(\langle \gamma \rangle^2 - 1)^{1/2}} \quad , \tag{6}$$

where n_i is the plasma ion density, $\underset{\sim}{v}$ the plasma fluid velocity, p the plasma pressure ($= (1 + Z)n_i kT$), $\mathcal{E}$ the total plasma energy density, and $\underset{\sim}{j}$ the plasma current. The following Maxwell equations close the above system when quasineutrality is assumed:

$$\underset{\sim}{\nabla} \times \underset{\sim}{E} = - \frac{\partial B}{\partial t} \quad , \tag{7}$$

$$\underset{\sim}{\nabla} \times \underset{\sim}{B} = 4\pi (\underset{\sim}{j} - en\underset{\sim}{u}) \quad . \tag{8}$$

The system of Eqs. (1) - (8) describes the full interaction of a relativistic electron beam with a plasma once the plasma-electron transport equations are included. Let us note at this point that the time-scales for the electron and ion dynamics are very different (of the order of 3 orders of magnitude) and constitute one of the major problems to the simultaneous solutions of these equations. Dealing with both scales in the same computer run would be costly and wasteful unless a quasi-static approach to solving the electron equations is attempted in order to eliminate the short time-step requirement imposed by the Courant condition. This is reasonable since relativistic electron transit times are much smaller than the time over which macroscopic quantities vary. Such a formulation is in development. Equations (1) - (8) can be

simplified depending on the region of the beam plasma interaction under investigation. In fact, the electron beam-anode plasma system can be separated into three regions. In the first region, the beam flows through a vacuum containing field-emitted ions from the anode[5] and is governed by the action of space-charge electric and magnetic fields and the applied axial accelerating field. In this region, Eqs. (1) - (3) apply with the coupling term set equal to 0 and E determined from Poisson's equation. In Region II, the beam interacts collectively with a low density plasma with diffusion of the magnetic field determined by the plasma conductivity in that region. In Region III, the beam interacts collisionally with the high-density plasma produced near the anode surface. The full system of Eqs. (1) - (8) apply in that region where collisions dominate. However, the action of dynamic friction which broadens the beam energy distribution is difficult to determine without recourse to kinetic theory.[6,7]

In this work, we limit consideration to Region II where both quasineutrality and no collisions can be assumed. In that region where collisions are not important but where the field diffuses, the full system of equations can be reduced to the following:

$$\frac{\partial n}{\partial t} + \nabla \cdot n\underset{\sim}{u} = 0 \,, \tag{9}$$

$$\frac{\partial \underset{\sim}{u}}{\partial t} + \underset{\sim}{u} \cdot \nabla \underset{\sim}{u} + \frac{e}{m_o \gamma} \left[\underset{\sim}{E} \cdot \left(\underset{\approx}{I} - \frac{\underset{\sim}{u}\underset{\sim}{u}}{c^2} \right) + \underset{\sim}{u} \times \underset{\sim}{B} \right] = 0 \,, \tag{10}$$

$$\nabla \times \underset{\sim}{E} = - \frac{\partial \underset{\sim}{B}}{\partial t} \quad , \tag{11}$$

$$\nabla \times \underset{\sim}{B} = 4\pi (\underset{\sim}{j} - en\underset{\sim}{u}) \quad . \tag{12}$$

In these equations, it has been assumed that the ion dynamics is frozen and only the beam equations and Maxwell equations are solved for. The plasma conditions enter these equations through an assumed constant scalar conductivity

$$\underset{\sim}{j} = \sigma \underset{\sim}{E} \quad .$$

Furthermore, it is assumed that the electron beam is cold (i.e. the pressure term is equal to 0) since the beam-plasma collisions are negligible. As a result, the energy of the beam shows only in kinetic form and remains unchanged $\left(\text{i.e. changes in electric potential inside the plasma} \ll \frac{m_o c^2}{e}\right)$ so that the beam energy equation is not required any more. Equations (11) - (12) can be shown to constitute the diffusion equation for the magnetic field. In Eq. (12), $\underset{\sim}{j}_b = - en\underset{\sim}{u}$ is the primary current and $\underset{\sim}{j} = \sigma \underset{\sim}{E}$ is the plasma current. Note that when $\underset{\sim}{j}_b = - \underset{\sim}{j}$, the total current is 0 and we have

$$\nabla \times \underset{\sim}{B} = 0 \quad .$$

The initial and boundary conditions are the following. At t = 0 and z = 0 (which delimits the beginning of Region II), the beam front enters the low density anode plasma. In that plane, the magnetic field

is the self field of the beam, i.e., $B(r, 0, t) = B_o$ and remains so at all times. For $z > 0$, $B(r, z, 0) = 0$ so that initially the total current vanishes. This condition will in turn impose an electric field E_o defined by

$$E_o = - \eta e n(r, 0, 0)\, u_z(r, 0, 0) ,$$

where u_z is given by the initial choice of γ and $\eta = \sigma^{-1}$. Care must be taken to make the velocity distribution of the beam consistent with the initial electric field in the plasma and so, initially we solve Eq. (13) for γ

$$\frac{d\gamma}{dz} = - \frac{E_o}{m_o c^2} . \tag{13}$$

From the continuity equation, it follows that

$$n(r, z, 0) = \frac{n(r, 0, 0)\, u_z(r, 0, 0)}{\sqrt{1 - \gamma(z)^{-2}}} .$$

The initial electron beam density distribution in the radial direction is chosen as a square profile whose edge has been smoothed slightly for computational purposes. The vacuum density outside the beam has been chosen to be 10^{-4} times the initial beam density for the present calculations, but it can be changed easily. The radial velocity u_r has been taken equal to 0 everywhere at $t = 0$. The radial electric field is assumed to be 0 at $z = L$ where L delimits the end of Region II. This condition results from the assumption that the anode is an equipotential plane.

Another characteristic of the model is that σ, the only quantity characterizing the plasma in the equations solved, is assumed to be constant, corresponding to an isothermal plasma in Region II. For practical reasons, σ was chosen so that complete diffusion of the magnetic field occurs after a few hundreds of time steps. This requirement corresponded to a very low temperature of the plasma (10^{-1} eV and below). In reality, σ is determined from the plasma temperature achieved by electron-beam heating in Eq. (6).

Numerically, the grid has been chosen inhomogeneous in the r-direction in order to increase the numerical resolution near the axis. The spatial step goes from 0.1 cm near the axis to 8.6 cm in the vacuum. Equations (9) and (10) are solved explicitly using FCT[8] whereas the magnetic field diffusion equation is solved implicitly. The time-step is controlled by the Courant condition based on the electron fluid motion.

III. RESULTS

The case presented below corresponds to the following input parameters:

Beam radius	5 cm
Beam current	1 MA
Beam axial velocity	$\beta_z = \frac{v_z}{c} = 0.943$ ($\gamma = 3$)
Length of Region II	0.5 cm

Figures 1 and 2 show density contours at $t = \tau_{diff}/2$ and $t = 2\ \tau_{diff}$ respectively where

$$\tau_{diff} = \frac{4\pi\sigma L^2}{c^2} .$$

The initial density was set equal to 2.8×10^{12} and remains so in the plane $z = 0$. Figure 1 shows pinch formation occurring obliquely with respect to the diode axis. The maximum density at the time of Fig. 1 is 2×10^{13}, almost an order of magnitude above the initial density. Figure 2 shows strong pinching on the axis near $z = L$. The density is then almost 200 times the initial density.

Figures 3 and 4 show e-beam fluid streak lines at the same times as Figs. 1 and 2. The pinching is seen to form closer to the end of Region II as the radius decreases. As time develops, this remains true but the pinching recedes toward the cathode. Outside the pinching region, we note areas where deconfining forces dominate temporarily.

The magnetic field at $r = 3.21$ cm is shown in Fig. 5. It is clear from this graph that the field excluded initially progressively fills the plasma in Region II. By $t = 2\ \tau_{diff}$, the field has diffused entirely into the anode plasma.

Figures 6 and 7 show radial profiles of the magnetic field at $t = \tau_{diff}/2$ and $t = 2\ \tau_{diff}$. At $z = 0$, the self-field of the beam is shown, increasing linearly with r up to the beam boundary and then decaying as $1/r$ in the vacuum. Departures from the linear rise indicates a higher current density near the axis, corresponding to pinching. This pinching is shown very clearly at $z = L$ in Fig. 7. The beam axial

velocity is down by more than a factor of 10 in this area. One of the results found with our model is that no steady state has been reached after 2 τ_{diff} and the flow remains unsteady in all parts of the Region II of the diode under consideration.

IV. CONCLUSIONS

In this work, we have described the electromagnetic interaction of a relativistic e-beam with an anode plasma. We have shown the solution in the low-density plasma region where fields diffuse but where collisions are unimportant. We have found that the beam pinches in such a configuration but that the solution does not reach a steady-state for the time-scales involved in this study. This is in part due to the fact that the plasma does not respond to beam-heating so that magnetic diffusion continues to larger values of z. If the plasma was allowed to heat, high temperature in the pinch would stop the diffusion. In any case, the pinching observed in the regime under investigation is significant because it shows that a low density plasma in front of the anode can cause its formation.

The discussed solution constitutes a first step in the solution of a full beam-plasma dynamic interaction. The relativistic e-beam fluid equations have been tested as well as the magnetic field diffusion equation. Addition of a pressure term to the beam equations and collisional coupling to a plasma system of equations remain to be done. In view of the length of the calculations required for the e-beam dynamics when performed on an electron time-scale, this study strongly suggests that the beam equations be solved implicitly if coupling to a much slower

dynamics is planned as a next step. Nevertheless, this study has provided interesting results of its own and pointed out causes of eventual problems in an implicit treatment.

V. REFERENCES

1. J. W. Poukey, J.R. Freeman, and G. Yonas, J. Vac. Sci. Tech. 10, 954 (1973).
2. S. A. Goldstein, R. C. Davidson, J. G. Siambis and R. Lee, Phys. Rev. Lett. 33, 1471 (1974).
3. S. Miller and Z. Zinamon, Phys. Rev. Lett. 36, 1303 (1976).
4. D. Mosher, Phys. of Fluids 18, 846 (1975).
5. S. A. Goldstein and R. Lee, Phys. Rev. Lett. 35, 1079 (1975).
6. D. Mosher, Phys. Rev. Lett. 35, 851 (1975).
7. D. Mosher and I. B. Bernstein, submitted to Phys. Rev. Lett.
8. J. Boris and D. Book, J. Comp. Phys. 11, 38 (1973).

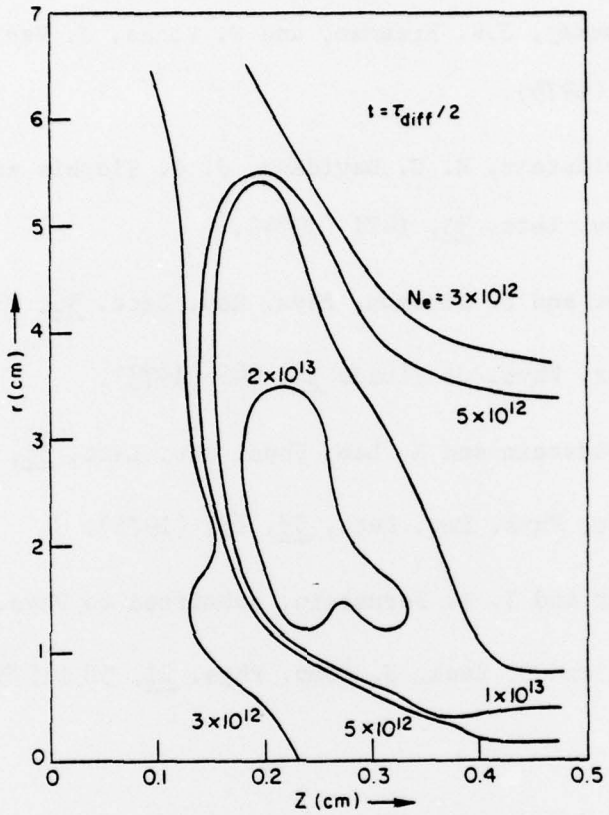

Fig. 1 — Electron density contours at $t = \tau_{diff}/2$ where τ_{diff} is the characteristic magnetic field diffusion time

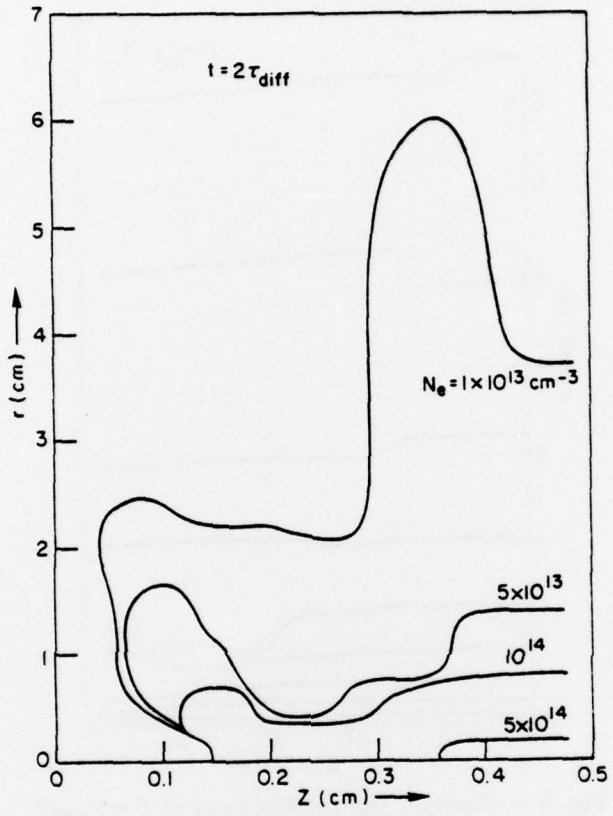

Fig. 2 — Electron density contours at t = 2 τ_{diff}

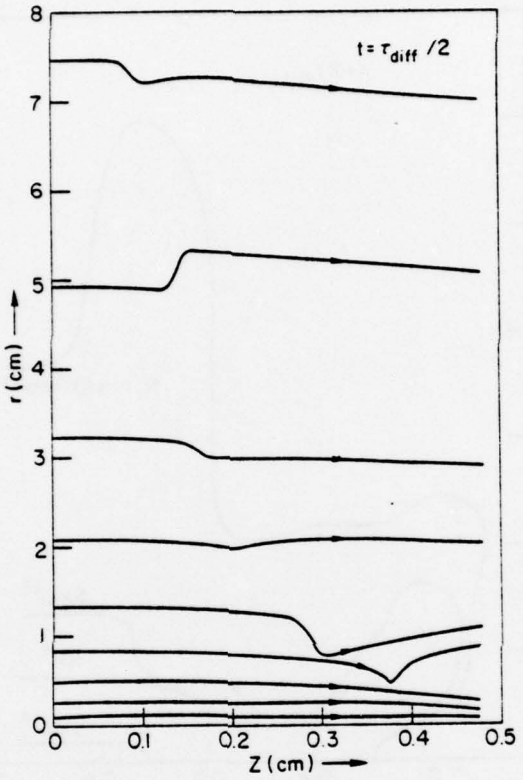

Fig. 3 — Electron fluid streak lines at t = $\tau_{diff}/2$

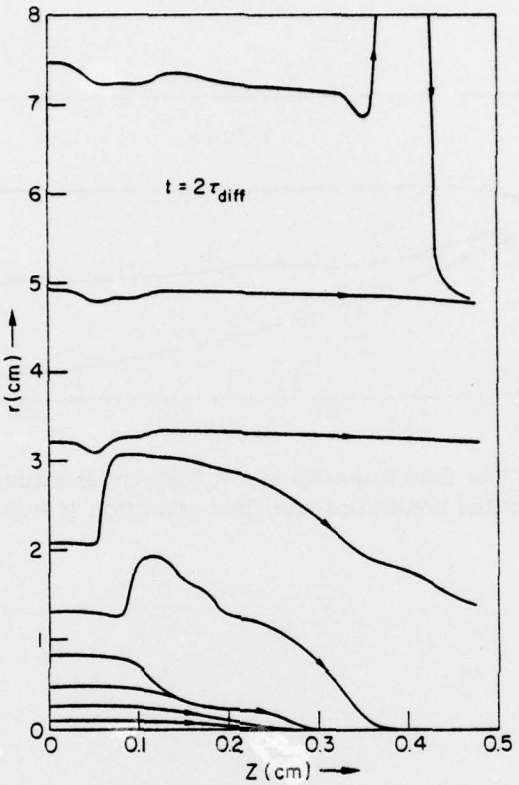

Fig. 4 — Electron fluid streak lines at $t = 2\,\tau_{diff}$

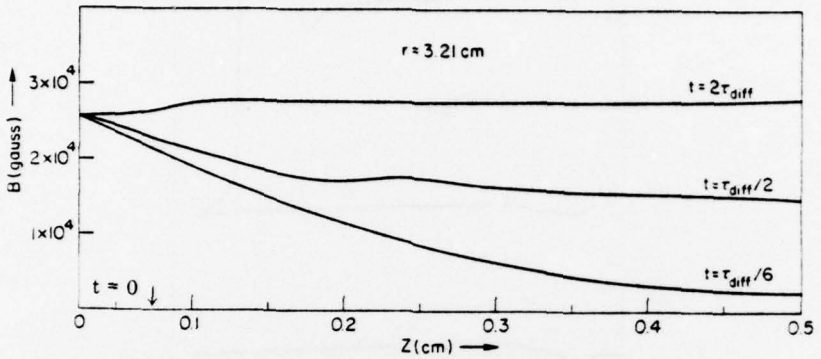

Fig. 5 — Magnetic field intensity at r = 3.21 cm as a function of time. Note initial conditions and final condition ($t = 2\ \tau_{diff}$).

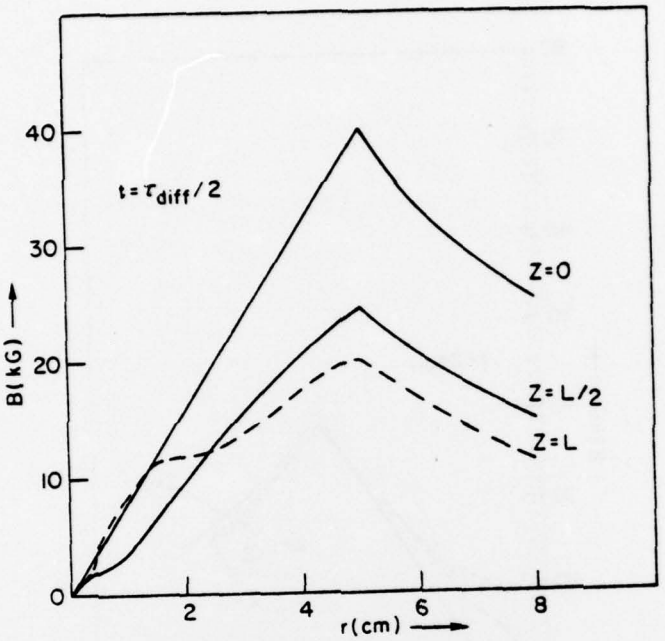

Fig. 6 — Magnetic field radial profiles at $t = \tau_{diff}/2$ at various z

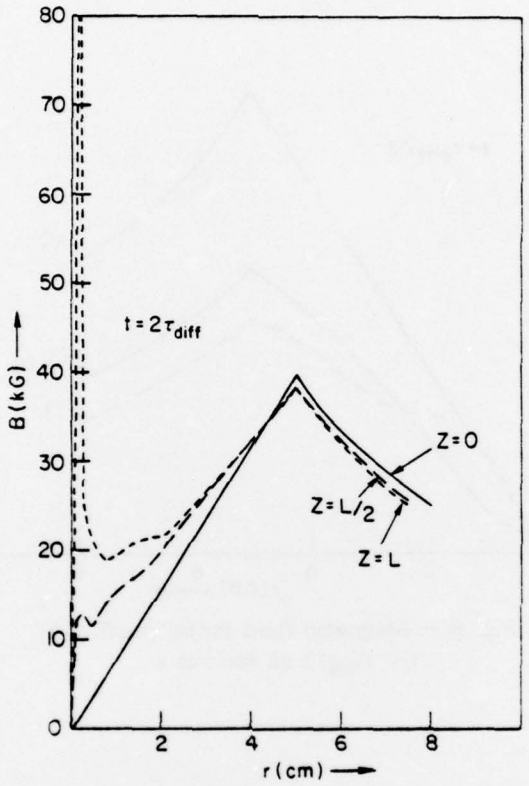

Fig. 7 — Magnetic field radial profiles at t = 2 τ_{diff} at various z. Note that at z = 0, the B field radial profile does not change. Also, large values of field near axis indicate pinching.

DISTRIBUTION LIST

1. Director
Defense Advanced Research Projects Agency
Architect Building
1400 Wilson Boulevard
Arlington, Virginia 22209
Attn: LTC R. P. Sullivan

2. Director
Defense Nuclear Agency
Washington, D. C. 20305
Attn: DDST, Mr. Peter Haas
RATN
STTL, Technical Library (2 copies)
RAEV (2 copies)
STVL
STSI

3. Commander
Field Command
Defense Nuclear Agency
Albuquerque
Kirtland AFB, New Mexico 87115
Attn: FCPR

4. Chief
Field Command
Defense Nuclear Agency
Livermore Division
Box 808
Livermore, California 94550
Attn: FCPR-L

5. Director
Defense Research and Engineering
Washington, D. C. 20301
Attn: DAD (SK) Mr. G. R. Barse

6. Commander
Harry Diamond Laboratories
Adelphi, Maryland 20783
Attn: AMXDO-RBF, Mr. John Rosado
AMXDO-RBH, Mr. S. Graybill
AMXDO-RC, Dr. Robert Oswald, Chief, LAB 300

7. Air Force Weapons Laboratory, AFSC
Kirtland AFB, New Mexico 87117
Attn: DY, Dr. Guenther
EL, Mr. John Darrah
DYS, Dr. Baker
SAA
SUL, Technical Library
ELP, TREE Section

8. Space and Missile Systems Organization
Post Office Box 92960
Worldway Postal Center
Los Angeles, California 90009
Attn: SKT, Mr. Peter H. Stadler
RSP, System Defense and Assessment, LTC Gilbert

9. Sandia Laboratories
P. O. Box 5800
Albuquerque, New Mexico 87115
Attn: Document Control for 5220, Dr. J. V. Walker
Document Control for 5242, Dr. G. Yonas
Document Control for Technical Library

10. Aerospace Corporation
P. O. Box 92957
Los Angeles, California 90009
Attn: Mr. J. Benveniste
Dr. Gerald G. Comisar, Jr.

11. University of Texas
Fusion Research Center
Physics Building 330
Austin, Texas 78712
Attn: Dr. William E. Drummond

12. Battelle Memorial Institute
Columbus Laboratories
505 King Avenue
Columbus, Ohio 43201
Attn: Mr. P. Malozzi

13. Maxwell Laboratories, Inc.
9244 Balboa Avenue
San Diego, California 92123
Attn: Dr. P. Korn

14. Mission Research Corporation
735 State Street
Santa Barbara, California 93101
Attn: Dr. Conrad L. Longmire

15. Physics International Corporation
2700 Merced Street
San Leandro, California 94577
Attn: Document Control for Dr. Sidney Putnam
Document Control for Mr. Ian Smith

16. R & D Associates
P. O. Box 9695
Marina del Rey, California 90291
Attn: Dr. Bruce Hartenbaum

17. Science Applications, Inc.
P. O. Box 2351
La Jolla, California 92037
Attn: Dr. J. Robert Beyster

18. Stanford Research Institute
333 Ravenswood Avenue
Menlo Park, California 94025
Attn: Dr. Robert A. Armistead, Jr.

19. Dr. Victor A. J. Van Lint
Mission Research Corporation
7650 Convoy Court
San Diego, California 92111

20. Commander
Naval Surface Weapons Center
White Oak Laboratory
Silver Spring, Maryland 20910

21. DASIAC, GE Tempo
El Paseo Building
816 State Street
Santa Barbara, California 93102

22. DDC (2 copies)

23. Code 2628 (20 copies)

24. Code 7700

25. Code 7770 (20 copies)